Available online at www.sciencedirect.com
ScienceDirect
Trans. Nonferrous Met. Soc. China 21(2011) 1105−1111
Transactions of Nonferrous Metals Society of China
www.tnmsc.cn

Ageing process of pre-precipitation phase in $Ni_{0.75}Al_{0.05}Fe_{0.2}$ alloy based on phase field method

DONG Wei-ping[1], WANG Yong-xin[1], CHEN Zheng[1, 2], YANG Kun[1]

1. College of Materials Science and Engineering, Northwestern Polytechnical University, Xi'an 710072, China;
2. State Key Laboratory of Solidification Processing, Northwestern Polytechnical University, Xi'an 710072, China

Received 10 May 2010; accepted 9 September 2010

Abstract: By utilizing phase field method combined with analysis on free energy and interatomic potentials, pre-precipitation phase formation and transformation process of $Ni_{0.75}Al_{0.05}Fe_{0.2}$ alloy in early precipitation stage during the ageing process under 1 000 K were studied. And free energy, microstructures, compositions and volume fractions of pre-precipitation phase and equilibrium phase were analyzed. The simulation results indicate that nonstoichiometric $L1_0$ pre-precipitation phase formed first, and then would gradually transform into $L1_2$ equilibrium phase. It is discovered that the phase transformation process was closely related to free energy and interatomic potentials. Additionally, it is revealed that free energy of $L1_0$ pre-precipitation phase was higher and interatomic potential was smaller than that of $L1_2$ equilibrium phase. Therefore, it is concluded that $L1_0$ phase was unstable, and phase transformation would occur to $L1_2$ which was more stable.

Key words: pre-precipitation phase; equilibrium phase; interatomic potentials; free energy; phase field method

1 Introduction

The precipitate transformation in precipitation process is regulated by atomic diffusion. Therefore, a series of metastable phases could probably be formed in this process[1]. To date, the diffusive phase transitions only include equilibrium phases. But some physical changes that preceded the formation of equilibrium phases determine the structures and properties to a certain extent, which is also instructive to practical production. Thereby, investigations on them have attracted attention for many years[2−3]. Al-Cu alloy series had been studied most extensively[4−5]. Metastable or transitional nonequilibrium phases precipitate first when alloys quickly cool off from single-phase region to double-phase region[6]. And these nonequilibrium phases are called 'pre-precipitation phase'. However, this process is so transient that it can be finished instantaneously. Therefore, it is difficult to conduct an investigation by conventional experimental methods. LI et al[7] prepared Cu-1.56Cr alloy powder by utilizing fog test and implemented ageing at 500 °C. And it was found that there were two modulated metastable structures which could offer structural transition from FCC oversaturation solid solution to BCC precipitated phase. TAWANCY and ABOELFOTOH[8] discovered that there are $D0_{22}$ and $D1_a$ super-structure as a transitional metastable phase in Ni_2(Cr, Mo) evolving with time during ageing process using TEM images. In relation to the temporal and spatial scales of alloy in early precipitation stage, the temporal one is in time-scale of seconds and the spatial one stays in volume-scale of ten to hundred atoms. Therefore, it forms nano-scale dispersion strengthening phase. It is necessary to employ computer simulations to analyze patterns in early precipitation stage of alloys because existing measurements are insufficient and incapable of examining them thoroughly. In terms of computer simulations, CHEN and KHACHATURYAN[9] utilized microscopic phase field method to simulate alloys and discovered the probable existence of virtual ordered phase during the transformation process from evenly disordered phase to double equilibrium phase. REINHARD and TURCHI[10] found that B32 transitional ordered phase would appear when the

Foundation item: Projects(10902086, 50941020, 50875217) supported by the National Natural Science Foundation of China; Projects(JC201005) supported by Basic Research Fund of Northwestern Polytechnical University, China; Project supported by Graduate Starting Seed Fund and Doctoral Foundation of Northwestern Polytechnical University, China
Corresponding author: DONG Wei-ping; Tel: +86-29-88486023; E-mail: penny1688@gmail.com
DOI: 10.1016/S1003-6326(11)60828-5

quenched solid solution was dissolved into Ti-and V- rich disordered phase with Monte-Carlo method. SOISSON and MARTIN[11] studied the decomposition of the instantaneous nucleation and the steady-state nucleation dynamics of metastable solution with Monte Carlo method. NI et al[12−14] found that nonequilibrium phase of quenched alloy turned to equilibrium ordered phase during the ordering process with microscopic master equation. TSAO et al[15] made quantitative analysis on natural ageing of Al-Mg-Si alloy with continuous heating and reciprocal transformation between metastable phase β'' and β' during the subsequent isothermal aging process by integrating SAXS, TEM and the numerical simulation of the classical theory.

The microscopic phase field adopted in this study is a type of deterministic phase field method which is capable of describing all diffusion processes, including atomic clustering, ordering, crystal boundary migration, growing up and coarsening of new phase, and formation of transient phase. In addition, this model can reproduce microstructures, compositions and order degree changes of the system in early precipitation stage thoroughly. So it has shown a great advantage in the study of pre-precipitation phase. MIAO et al[16] and ZHAO et al[17] found that pre-precipitation phase $L1_0$ would separate out during ageing process of $Ni_{80}Al_{13}Cr_7$ and $Ni_{75}Al_{17}Zn_8$ alloys by this model. Free energy is based on continuous medium. And many previous investigations used it to discuss and explain the various phenomena of micro-organizational processes, but it had been proven to be very limited in atomic simulation. Since the interatomic potentials are the basis of computer simulation on properties and processes of atomic condensed matters, it is quite reasonable to study the process of precipitation by combining free energy and interatomic potentials.

2 Theoretical models

2.1 Microscopic phase field model

The phase field dynamic equation is based on the Onsager and Ginzburg-Landau theories, which describe atomic configuration and the precipitation pattern of the ordered phases by the occupation probability $P(\boldsymbol{r}, t)$ at the crystal lattice site $\boldsymbol{r}$ and the time t, whose change rate is proportional to the variation of free energy. The kinetic equation is written as

$$\frac{\partial P(\boldsymbol{r},t)}{\partial t}=\sum_{\boldsymbol{r}'}L(\boldsymbol{r}-\boldsymbol{r}')\frac{\delta F}{\delta P(\boldsymbol{r}',t)} \tag{1}$$

For ternary system, atomic occupation probabilities satisfy

$$P_{\mathrm{A}}(\boldsymbol{r},t)+P_{\mathrm{B}}(\boldsymbol{r},t)+P_{\mathrm{C}}(\boldsymbol{r},t)=1 \tag{2}$$

where the subscripts A, B and C designate three kinds of atoms. In this simulation, it puts the simplification for crystalline defects, but just considers the integrated lattice to response atomic diffusion. Therefore the equations can be obtained by

$$\begin{cases}\dfrac{\mathrm{d}P_{\mathrm{A}}(\boldsymbol{r},t)}{\mathrm{d}t}=\dfrac{1}{k_{\mathrm{B}}T}\sum\limits_{\boldsymbol{r}'}[L_{\mathrm{AA}}(\boldsymbol{r}-\boldsymbol{r}')\dfrac{\partial F}{\partial P_{\mathrm{A}}(\boldsymbol{r}',t)}+ \\ \qquad L_{\mathrm{AB}}(\boldsymbol{r}-\boldsymbol{r}')\dfrac{\partial F}{\partial P_{\mathrm{B}}(\boldsymbol{r}',t)}]+\zeta_1(\boldsymbol{r},t) \\ \dfrac{\mathrm{d}P_{\mathrm{B}}(\boldsymbol{r},t)}{\mathrm{d}t}=\dfrac{1}{k_{\mathrm{B}}T}\sum\limits_{\boldsymbol{r}'}[L_{\mathrm{BB}}(\boldsymbol{r}-\boldsymbol{r}')\dfrac{\partial F}{\partial P_{\mathrm{B}}(\boldsymbol{r}',t)}+ \\ \qquad L_{\mathrm{AB}}(\boldsymbol{r}-\boldsymbol{r}')\dfrac{\partial F}{\partial P_{\mathrm{A}}(\boldsymbol{r}',t)}]+\zeta_2(\boldsymbol{r},t)\end{cases} \tag{3}$$

where $\zeta(\boldsymbol{r}, t)$ is the random noise term; $L(\boldsymbol{r}-\boldsymbol{r}')$ is the proportionality constant.

In the mean-field approximation, the free energy for ternary system is given by

$$\begin{aligned}F=&-\frac{1}{2}\sum_{\boldsymbol{r}}\sum_{\boldsymbol{r}'}\big[(-V_{\mathrm{AB}}(\boldsymbol{r}-\boldsymbol{r}')+V_{\mathrm{BC}}(\boldsymbol{r}-\boldsymbol{r}')+ \\ &V_{\mathrm{AC}}(\boldsymbol{r}-\boldsymbol{r}'))P_{\mathrm{A}}(\boldsymbol{r})P_{\mathrm{B}}(\boldsymbol{r}')+V_{\mathrm{AC}}(\boldsymbol{r}-\boldsymbol{r}')P_{\mathrm{A}}(\boldsymbol{r})\,P_{\mathrm{A}}(\boldsymbol{r}')+ \\ &V_{\mathrm{BC}}(\boldsymbol{r}-\boldsymbol{r}')P_{\mathrm{B}}(\boldsymbol{r})P_{\mathrm{B}}(\boldsymbol{r}')\big]+ \\ &k_{\mathrm{B}}T\sum_{\boldsymbol{r}'}\big[P_{\mathrm{A}}(\boldsymbol{r})\ln(P_{\mathrm{A}}(\boldsymbol{r}))+P_{\mathrm{B}}(\boldsymbol{r})\ln(P_{\mathrm{B}}(\boldsymbol{r}))+ \\ &(1-P_{\mathrm{A}}(\boldsymbol{r})-P_{\mathrm{B}}(\boldsymbol{r}))\ln(1-P_{\mathrm{A}}(\boldsymbol{r})-P_{\mathrm{B}}(\boldsymbol{r}))\big]\end{aligned} \tag{4}$$

where k_{B} is the Boltzmann constant; $V_{\mathrm{AB}}(\boldsymbol{r}-\boldsymbol{r}')$ is the effective interactive energy given as

$$V_{\mathrm{AB}}(\boldsymbol{r}-\boldsymbol{r}')=W_{\mathrm{AA}}(\boldsymbol{r}-\boldsymbol{r}')+W_{\mathrm{BB}}(\boldsymbol{r}-\boldsymbol{r}')-2W_{\mathrm{AB}}(\boldsymbol{r}-\boldsymbol{r}') \tag{5}$$

where W_{AA}, W_{BB}, W_{AB} are pairwise potentials between A and A, B and B, and A and B. In order to keep reliabilities of simulations, the fourth nearest-neighbor interaction is adopted. $V_{\mathrm{AB}}{}^1$, $V_{\mathrm{AB}}{}^2$, $V_{\mathrm{AB}}{}^3$, $V_{\mathrm{AB}}{}^4$ stand for the first-nearest, second-nearest, third-nearest and fourth-nearest interactive energies, respectively. Then substitute them into the FCC, reciprocal space:

$$\begin{aligned}V_{\mathrm{AB}}(\boldsymbol{k})=&4V_{\mathrm{AB}}^1[\cos(\pi h)\cdot\cos(\pi k)+\cos(\pi h)\cdot\cos(\pi l)+ \\ &\cos(\pi k)\cdot\cos(\pi l)]+2V_{\mathrm{AB}}^2[\cos(2\pi h)+ \\ &\cos(2\pi k)+\cos(2\pi l)]+8V_{\mathrm{AB}}^3[\cos(2\pi h)\cdot \\ &\cos(\pi k)\cdot\cos(\pi l)+\cos(\pi h)\cdot\cos(2\pi k)\cdot \\ &\cos(\pi l)+\cos(\pi h)\cdot\cos(\pi k)\cdot\cos(2\pi l)]+ \\ &4V_{\mathrm{AB}}^4[\cos(2\pi h)\cdot\cos(2\pi k)+ \\ &\cos(2\pi h)\cdot\cos(2\pi l)+\cos(2\pi k)\cdot\cos(2\pi l)]\end{aligned} \tag{6}$$

For

$$\boldsymbol{k}=(\boldsymbol{k}_x,\boldsymbol{k}_y,\boldsymbol{k}_z)=h\boldsymbol{a}_1^*+k\boldsymbol{a}_2^*+l\boldsymbol{a}_3^* \tag{7}$$

where k, h and, l are reciprocal lattice sites; $\boldsymbol{a}_1^*$, $\boldsymbol{a}_2^*$ and $\boldsymbol{a}_3^*$ are the unit reciprocal lattice vectors of the FCC

structure along three directions.

2.2 Interatomic potentials equations

The evaluation equations of interatomic potentials were initially proposed by KHACHATURYAN[18]. Based on concentration wave equations, the relational equations between occupation probability of solute atoms (B atoms) and free energy were deduced out:

$$c\left(1+\sum_{s=1}^{t-1}\eta_s E_s(r)\right)= \left[\exp\left(\frac{-\mu+c\cdot V(0)-c\cdot V(k_s)\cdot\eta_s E_s(r)}{k_{\mathrm{B}}T}\right)+1\right]^{-1} \tag{8}$$

where c is atomic concentration of solute atoms (B atoms); η_s corresponds to long range order parameter; $E_s(r)$ denotes a function associated with lattice symmetry; μ means chemical potential between atoms; $t-1$ indicates the number of non-zero vector $\boldsymbol{k}_s$ in superlattice structure, with k_{B} being the Boltzmann constant; T is temperature; $V(0)$ is potential energy of disordered atoms.

There are two occupations of $L1_2$ phase: $c(1+3\eta)$ and $c(1-\eta)$. The equation between the first nearest neighbor interatomic potential V_{AB}^1 of $L1_2$ phase and long range order parameter can be gained according to Eq.(8):

$$\frac{-4V_{\mathrm{AB}}^1\cdot\eta}{k_{\mathrm{B}}T}=\ln\frac{(1-\eta)[1-c(1+3\eta)]}{(1+3\eta)[1-c(1-\eta)]} \tag{9}$$

And $L1_0$ phase also has two occupations: $c(1+\eta)$ and $c(1-\eta)$. The equation between the first nearest neighbor interatomic potential V_{AB}^1 of $L1_0$ phase and long range order parameter also can be gained according to Eq.(8):

$$\frac{-4V_{\mathrm{AB}}^1\cdot\eta}{k_{\mathrm{B}}T}=\ln\frac{(1-\eta)[1-c(1+\eta)]}{(1+\eta)[1-c(1-\eta)]} \tag{10}$$

The first nearest neighbor interatomic potential V_{AB}^1 of $L1_2$ phase and $L1_0$ phase under varying temperature and atomic concentrations can be computed out by considering Eqs.(9) and (10). This study initiates simulations on $Ni_{0.75}Al_xFe_{0.25-x}$ alloy based on the aforementioned equations. They can overcome the deficiencies of conventional model ignoring the impact of temperature and concentrations, as well as using fixed interaction potential values in simulation computation.

3 Results

Due to the close connection between free energy and interatomic potentials of alloy in precipitation process, here we use atomic evolution maps, occupation probabilities and volume fractions to study this type of connection. Using the calculated interatomic potentials at 1 000 K, the atomic evolution maps of $Ni_{0.75}Al_{0.05}Fe_{0.2}$ alloy with varying time step are illustrated in Fig.1, in which the black parts indicate Ni basal body and white parts correspond to Al(Fe) atoms. The $L1_0$(Ni-Al(Fe)) phases and $L1_2$(Ni-Al(Fe)) phases gained during the precipitation process of alloy are marked in the maps. The map is totally gray when the time step is 10, which indicates the basal body is in complete disorder, as shown in Fig.1(a). As time goes by, many ordered phases separate out. When time step increases to 1 200, a few $L1_0$(Ni-Al(Fe)) phases while only a small amount of $L1_2$(Ni-Al(Fe)) phases appear. And Fig.1(c) demonstrates that $L1_0$(Ni-Al(Fe)) phases start to transform into $L1_2$(Ni-Al(Fe)) phases when time step is 1 500, which testifies the fact that pre-precipitation phases $L1_0$ are quite unstable and their existences are very transient. In Fig.1(d), $L1_2$(Ni-Al(Fe)) phases have already occupied the whole evolution map when time step is 2 000. And most ordered $L1_2$(Ni-Al(Fe)) phases are interconnected, which means that $L1_0$(Ni-Al(Fe)) phases have already transformed into $L1_2$(Ni-Al(Fe)) phases completely. When time step reaches 10 000, as illustrated in Fig.1(e), the previous ordered phases gradually grow up and form into the stoichiometric order phase of $L1_2$ phases. With time step of 200 000, Fig.1(f) shows that occupation probabilities of atoms in corresponding lattice have ultimately arrived at their equilibrium values, and $L1_2$ phases coarsen. The above results are consistent with the precipitation process, which fully indicates that corresponding phase transformation outcomes could be gained by employing interatomic potentials obtained from equation calculations to model the microscopic phase field. And the $L1_2$ phases in Fig.1(e) match well with the experimental results by HIMURO et al[19].

From the evolution maps, we know that there are pre-precipitation phases $L1_0$ in the precipitation process of $Ni_{0.75}Al_{0.05}Fe_{0.2}$ alloy. In order to further clarify the early precipitation effects and the transformation process of equilibrium phase, we analyzed the two-dimensional atomic structure and the evolution maps changing with time step shown in Fig.2 and the occupation probability curves shown in Fig.3. Among them, Fig.2(a) shows $L1_0$ atomic structure and related atomic evolution map of phase, in which the indices (lattice positions) α, β and γ in atomic structure correspond to the same indices in the evolution map. Similarly, Fig.2(b) means the atomic structure and related atomic evolution map of $L1_2$ phase. Specifically, the indices in Fig.2(a) and Fig.2(b) indicate the same lattice position. As seen from the Fig.2(a) and Fig.2(b), the element in lattice position α is black Ni all the time; the element of lattice position β in Fig.2(a) is white Al(Fe), but it is replaced by black Ni in Fig.2(b); white Al(Fe) occupies lattice position γ all along, but it

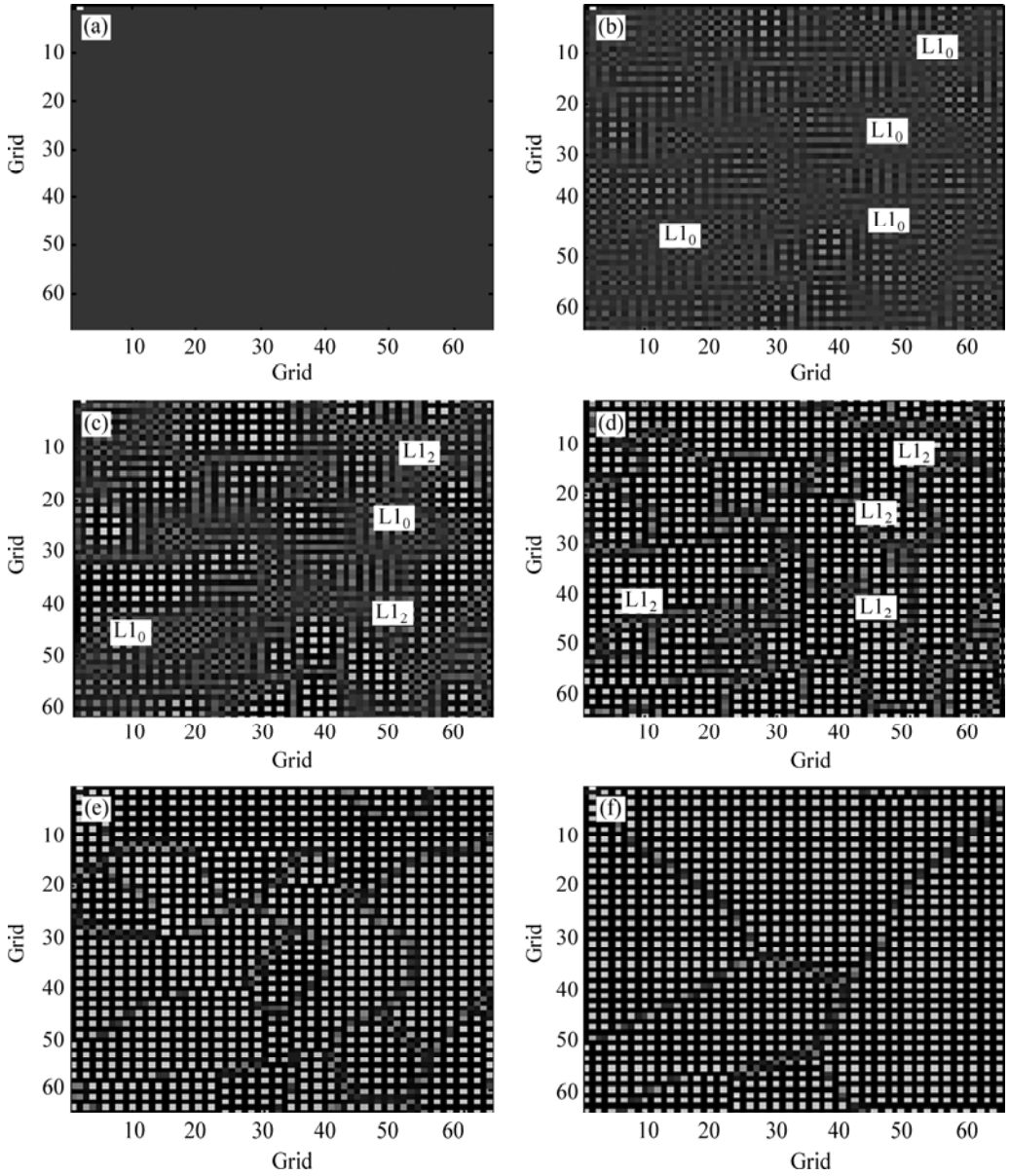

Fig.1 Temporal atomic evolution maps of $Ni_{0.75}Al_{0.05}Fe_{0.2}$ alloy at 1 000 K: (a) *t*=10 step; (b) *t*=1 200 step; (c) *t*=1 500 step; (d) *t*=2 000 step; (e) *t*=10 000 step; (f) *t*=200 000 step

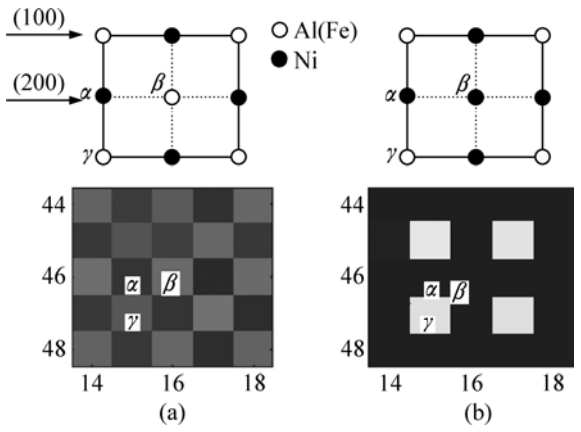

Fig.2 Atomic structure and simulated evolution maps: (a) *t*=1 200 step, $L1_0$ phase; (b) *t*=2 000 step, $L1_2$ phase

whitens more and transforms from equilibrium phase to stoichiometric structure as time step increases. These correspond to atomic structures of pre-precipitation phase $L1_0$ (Ni-Al (Fe)) and equilibrium phase $L1_2$ (Ni-Al(Fe)).

The atomic structure transformation processes demonstrated by Fig.2 is inadequate to further specifically study the transformation status of occupation probabilities at each lattice position. The atomic occupation probability (concentration) variation curves shown in Fig.3 must be incorporated, in which the solid line corresponds to occupation of Ni atoms, the long-dashed line means occupation of Fe atoms and the dashed line denotes occupation of Al atoms. Fig.3(a) indicates the atomic occupation probability changes with

time step variance at lattice position α in Fig.2. It is obvious that Ni atomic occupation probability increases up to near 1 while both Fe and Al decrease to around 0. Thus it is consistent with the fact that Ni atoms occupy lattice position α all the time. Figure 3(b) shows the atomic occupation probability at lattice position β in Fig.2. It is indicated that occupation probability of Ni atoms first goes down to near 0.5 and then increases to around 1, but Fe and Al first increase to near 0.5 and then decrease to around 0. Therefore, $L1_0$ phase does not arrive at stoichiometric structure. This is in line with the change in lattice position β from Fig.2(a) and Fig.2(b), which signifies that Al(Fe) atoms will be replaced by Ni atoms. That is, the transitional pre-precipitation phases $L1_0$(Ni-Al(Fe)) exist. Similarly, Fig.3(c) corresponds to the atomic occupation probability at lattice position γ in Fig.2. It is represented that occupation probabilities of Ni atoms keep getting down to near 0, while occupation probabilities of Fe and Al atoms maintain increasing till around 1, which is corresponding to changes at lattice position γ from Fig.2(a) and Fig.2(b). They could explain the fact that Al(Fe) atoms occupy lattice position γ all the time until they reach equilibrium phase $L1_2$.

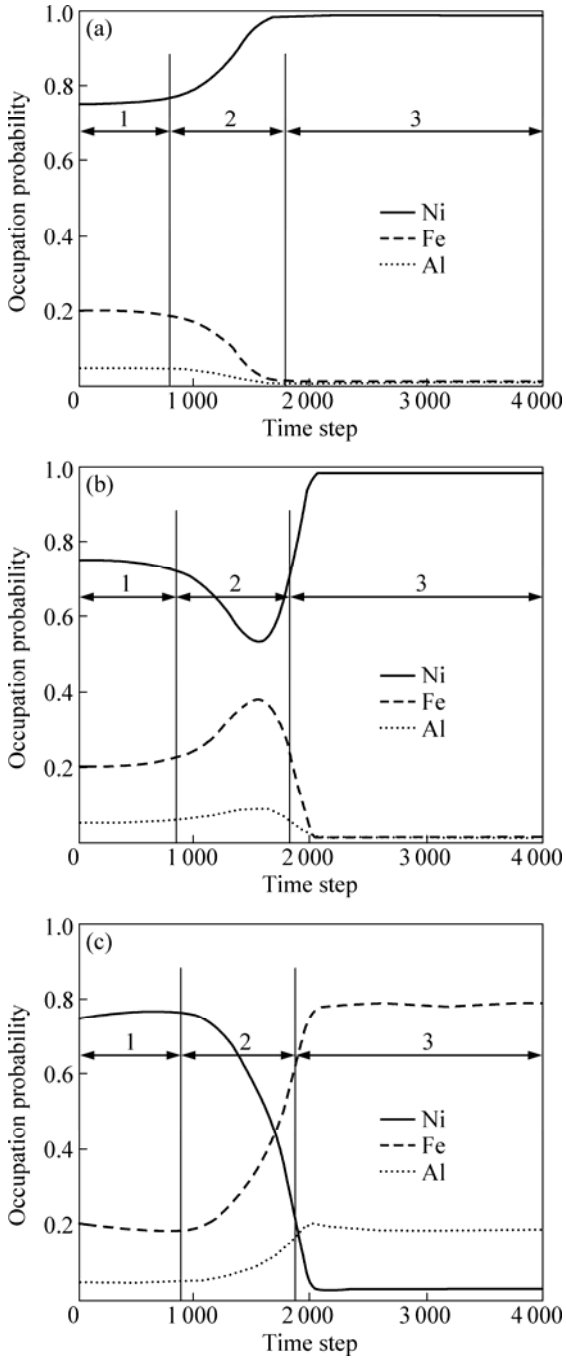

Fig.3 Occupation probability changes with time step: (a) α lattice; (b) β lattice; (c) γ lattice (1—Gestation of disordered basal body; 2—Migration process of disordered phase to pre-precipitation $L1_0$ phase, and $L1_0$ phase migrates into equilibrium $L1_2$ phase; 3—Coarsening and growing-up process of $L1_2$ phase)

Before lattice positions α and β come to equilibrium phases, reduction occupation probabilities of Al(Fe) atoms corresponds to the increase of lattice position γ. This denotes the migration of Al(Fe) atoms during the precipitation process; the increase of occupation probabilities of Ni atoms before lattice α and β reaches equilibrium phases and means the reduction of lattice position γ, which indicates that migration of Ni atoms could also occur in precipitation process. Moreover, the migration process is in correspondence with such procedure: disordered phase→pre-precipitation phase $L1_0$(Ni-Al(Fe))→equilibrium phase $L1_2$(Ni-Al(Fe)). This procedure is illustrated by sections 1, 2 and 3 in the curve in Fig.3, respectively.

The alloy volume fraction curves of precipitation phases are shown in Fig.4. Obviously, between the 1 000th and 2 000th step $L1_0$ phase increases rapidly, which also shows the existence of pre-precipitation phase $L1_0$. And a sharp reduction after that indicates that $L1_0$ phase changes to equilibrium phase $L1_2$. The curve of $L1_2$ phase increases after the step 2 000, which means the $L1_2$ phase forms until the step 2 000.

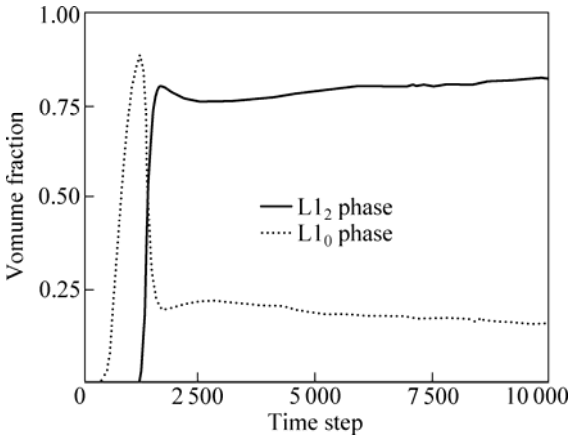

Fig.4 Volume fractions of different phases with time steps

4 Discussion

Studies found that parent phase usually could not transform into the lowest free energy equilibrium phase directly during the phase transition process. It turned into pre-precipitation phase of which the free energy was lower than parent phase but higher than equilibrium phase. This pre-precipitation phase is approximately comparable to crystal structures and chemical compositions with parent phase. In order to lower the interfacial energy between basal body and precipitant, pre-precipitation phase tends to possess similar structures with basal body. In the $Ni_{0.75}Al_{0.05}Fe_{0.2}$ alloy, the structure of $L1_0$ phase is more close to the structure of disordered basal body. Therefore, prior to the formation of $L1_2$ phase, $L1_0$ phase will be formed first. The curve of free energy calculated by Eq.(4) changes with the molar fraction shown in Fig.5(a). From Fig.5(a), free energy continues to lower from the disordered phase to the $L1_2$ phase, which means the pre-precipitation phase $L1_0$ is served as the transitional phase during the decreasing process of free energy, so the unstable $L1_0$ phase will transform to the $L1_2$ phase. Figure 5(b) demonstrates the interatomic potentials calculated by Eqs.(9) and (10) for different phases with varying long-range order parameters. They all could increase with the augmentation of long-range order parameter. It is obviously shown that, for each curve, the interatomic potentials first go up gradually with increasing long-range order parameter, and then skyrocket when the parameter approaches to 1. More specifically, the potential curve of $L1_0$ phase is in the bottom, which means that its potentials are the least in the alloy. All potential curves of $L1_2$ phase are higher than those of $L1_0$ phase, and with $L1_2$(Ni-Al(Fe)) on the top. The size relations of these potentials would affect the stability of pre-precipitation phase and equilibrium phase of alloy during the precipitation process. However, as seen from interatomic potentials curves in Fig.5(b), interatomic potentials of $L1_0$ are less than those of $L1_2$, which means that $L1_0$ phase is not as stable as $L1_2$ phase, and the pre-precipitation phase $L1_0$ will transform into equilibrium phase $L1_2$ that is more stable.

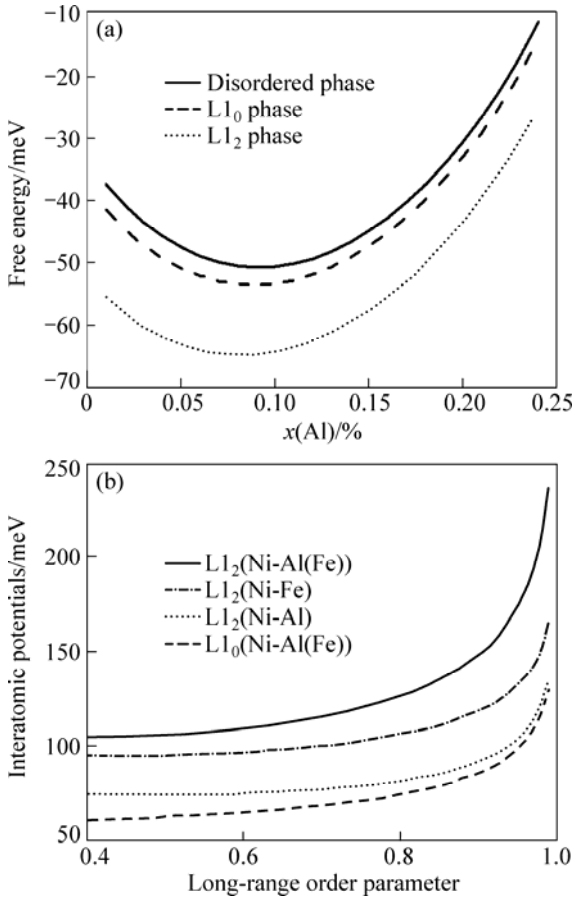

Fig.5 Free energy and interatomic potentials curves of different phases: (a) Free energy; (b) Interatomic potentials

5 Conclusions

1) Pre-precipitation phase $L1_0$ separates out before stable equilibrium phase $L1_2$ in $Ni_{0.75}Al_{0.05}Fe_{0.2}$ alloy. And as time goes by, this unstable transitional phase $L1_0$ will transform into equilibrium phase $L1_2$ that is more stable.

2) Due to the unstable property of transitional phase, pre-precipitation phase $L1_0$ cannot reach stoichiometric structure. However, equilibrium phase $L1_2$ is stable and can coarsen and grow up as time goes by. Therefore, it could arrive at stoichiometric structure.

3) Free energy lowers from the disordered phase to $L1_0$ phase to $L1_2$ phase. And the interatomic potentials of $L1_2$ phase are larger than those of $L1_0$ phase. Therefore, $L1_0$ phase is unstable, and will transform into $L1_2$ phase as time increases.

4) The precipitation sequence of $Ni_{0.75}Al_{0.05}Fe_{0.2}$ alloy is:

$$\text{disordered phase} \xrightarrow{\text{lower interfacial energy and similar structure}} L1_0 \text{ pre-precipitation phase} \xrightarrow{\text{lower free energy and larger interatomic potentials}} L1_2 \text{ equilibrium phase}$$

References

[1] BODEGA J, GARCÉS G, LEARDINI F, ARES J R, FERNÁNDEZ J F, ADEVA P, SÁNCHEZ C. A new metastable crystalline phase in the Cr-Zr system [J]. Intermetallics, 2010, 18: 1099−1101.

[2] SHI Hong-ting, NI Jun. Ordering and metastable state during the growth of fcc alloy monolayers [J]. Physical Review B, 2002, 65: 115422.

[3] MU Si-guo, CAO Xing-min, TANG Yu-qiong, XIANG Chao-jian, YANG Chun-xiu, GUO Fu-an, TANG Mo-tang. Microstructure and

properties of aging Cu-Cr-Zr-Mg-RE alloy [J]. The Chinese Journal of Nonferrous Metals, 2007, 17(7): 1112−1118. (in Chinese)
[4] HUANG L P, CHEN K H, LI S, SONG M. Influence of high-temperature pre-precipitation on local corrosion behaviors of Al-Zn-Mg alloy [J]. Scripta Materialia, 2007, 56: 305−308.
[5] CHEN Hui, LUO Ji-man, HAN Ze-guang, XU Xi-sha. Study on milling induced structural transformation in Al-Zn-Cu alloys[J]. Journal of Shenyang Jianzhu University: Natural Science, 2007, 23(4): 672−675. (in Chinese)
[6] WANG Zhen-ling, WANG Hong-wei, WEI Zun-jie, CAO Lei. High pressure solidification microstructure and stability of Al-9.6%Mg alloy [J]. The Chinese Journal of Nonferrous Metals, 2007, 17(3): 384−389. (in Chinese)
[7] LI Qiang, CHEN Jing-chao, SUN Jia-lin. The meta-stable structure of aging Cu-Cr alloy [J]. Rare Metals and Cemented Carbides, 2006, 34(4): 1−5. (in Chinese)
[8] TAWANCY H M, ABOELFOTOH M O. Application of long-range ordering in the synthesis of a nanoscale Ni2(Cr,Mo) superlattice with high strength and high ductility [J]. Materials Science and Engineering A, 2009, 500: 188−195.
[9] CHEN Long-qing, KHACHATURYAN A G. Formation of virtual ordered states along a phase-decomposition path [J]. Physical Review B, 1991, 44(9): 4681−4684.
[10] REINHARD L, TURCHI P E A. Transient ordered states in phase-separating alloys [J]. Physical Review Letters, 1994, 72(1): 120−123.
[11] SOISSON F, MARTIN G. Monte Carlo simulations of the decomposition of metastable solid solutions: Transient and steady-state nucleation kinetics [J]. Physical Review B, 2000, 62(1): 203−214.
[12] NI Jun, GU Bing-lin. Transient ordered states during relaxation from a quenched disordered state to an equilibrium disordered state [J]. Physical Review Letters, 1997, 79(20): 3922−3925.
[13] NI Jun, SHI Hong-ting, GU Bing-li. Kinetics of ordering for a ternary system on square lattice [J]. Physica A, 2002, 303: 397−409.
[14] NI Jun, GU Bing-lin. Kinetics of ordering in fcc alloys during codeposition [J]. Surface Science, 2002, 499: 174−182.
[15] TSAO C S, CHEN C Y, JENG U S, KUO T Y. Precipitation kinetics and transformation of metastable phases in Al-Mg-Si alloys [J]. Acta Materialia, 2006, 54: 4621−4631.
[16] MIAO Shu-fang, CHEN Zheng, WANG Yong-xin, XU Cong, MA Rui, ZHANG Ming-yi. Microscopic phase-field method simulation for the in situ transformation of $L1_0$ phase and $L1_2$ phase structure [J]. Acta Metallurgica Sinica, 2009, 45(5): 630−634. (in Chinese)
[17] ZHAO Yan, CHEN Zheng, LU Yan-li, ZHANG Li-peng. Microscopic phase-field study on aging behavior of $Ni_{75}Al_{17}Zn_8$ alloy [J]. Transactions of Nonferrous Metals Society of China, 2010, 20: 675−681.
[18] KHACHATURYAN A G. Theory of structural transformation in solids [M]. New York: Wiley, 1983.
[19] HIMURO Y, TANAKA Y, KAMIYA N, OHNUMA I, KAINUMA R, ISHIDA K. Stability of ordered $L1_2$ phase in Ni_3Fe-Ni_3X (X:Si and Al) pseudobinary alloys [J]. Intermetallics, 2004, 12(6): 635−643.

基于相场法的 $Ni_{0.75}Al_{0.05}Fe_{0.2}$ 合金预析出相时效过程

董卫平[1]，王永欣[1]，陈 铮[1,2]，杨 坤[1]

1. 西北工业大学 材料学院，西安 710072；
2. 西北工业大学 凝固技术国家重点实验室，西安 710072

摘要：用微观相场法结合自由能和原子间作用势研究了 $Ni_{0.75}Al_{0.05}Fe_{0.2}$ 合金在 1 000 K 时效中沉淀前期的预析出相的形成和转变过程；分析了沉淀前期预析出相和平衡相的自由能、微结构、成分和相体积分数随时间的变化。研究表明：由于结构接近，原子有序化首先形成非化学计量比预析出相 $L1_0$，随着时间的延长，预析出相 $L1_0$ 逐渐向 $L1_2$ 相转变，并逐渐达到化学计量比平衡相 $L1_2$。且发现此转变过程与自由能和原子间作用势有关，预析出相 $L1_0$ 比平衡相 $L1_2$ 的自由能高且原子间作用势小，故 $L1_0$ 相不稳定且转变为稳定的 $L1_2$ 相。

关键词：预析出相；平衡相；原子间作用势；自由能；相场法

(Edited by YANG Hua)